MicroRNA-96 promotes the proliferation and migration of breast cancer cells by inhibiting Smad7 expression

XIUMEI ZHANG[1], LIN CONG[1], RONG YU[2], QIANWEN YU[1], XIAN HOU[3] and YONGHUA ZHOU[4]

Departments of [1]Pathology, [2]Gastrointestinal Surgery, [3]Radiology and [4]Breast Surgery, The People's Hospital of Xinghua City, Xinghua, Jiangsu 225700, P.R. China

Received November 3, 2022; Accepted October 26, 2023

DOI: 10.3892/ol.2025.14897

Abstract. The present study aimed to investigate the effects of microRNA (miR)-96 on the proliferation and migration of breast cancer cells, and indicated that miR-96 may have a promoting role in breast cancer by inhibiting Smad7. Reverse transcription-quantitative (RT-q)PCR was used to detect the expression levels of miR-96 and Smad7 in breast cancer tissues and adjacent tissues. Western blotting and immunohistochemistry were conducted to determine the expression levels of SMAD7 in breast cancer and adjacent tissues. A dual luciferase assay was performed to verify the targeted binding between miR-96 and Smad7. Furthermore, the different expression patterns of miR-96 and Smad7 were compared in various breast cancer cell lines using RT-qPCR and western blotting. Among these cell lines, MDA-MB-231, which exhibited the highest expression of miR-96, was chosen for subsequent functional verification. The expression levels of miR-96 were significantly higher in breast cancer tissues compared with those in adjacent tissues. By contrast, the expression levels of Smad7 were significantly lower in breast cancer tissues compared with those in adjacent tissues. The dual luciferase assay revealed a targeted binding effect between miR-96 and Smad7. Notably, transfection with miR-96-5p mimics and short hairpin RNA-Smad7 markedly promoted the proliferation, adhesion, invasion and migration of breast cancer cells. Conversely, transfection with a miR-96-5p inhibitor and Smad7 overexpression plasmid exhibited the opposite trend. In conclusion, the expression levels of miR-96 were significantly elevated in breast cancer tissues compared with those in adjacent tissues. Overexpression of miR-96 was shown to promote the migration of breast cancer cells by downregulating the expression of Smad7. These findings indicated that miR-96 may serve as a prognostic marker for breast cancer.

Correspondence to: Dr Yonghua Zhou, Department of Breast Surgery, The People's Hospital of Xinghua City, 419 Yingwu Road South, Xinghua, Jiangsu 225700, P.R. China
E-mail: 13815912936@163.com

Key words: breast cancer, migration, signal transduction

Introduction

Breast cancer is the second leading cause of cancer-related death globally and remains the most common malignancy among women worldwide (1,2). Breast cancer is a highly heterogeneous disease. Previous studies have shown that early diagnosis and timely treatment can significantly improve the prognosis and increase the survival time of patients with breast cancer (3,4). At present, mammography and ultrasound imaging are widely used for early breast cancer screening (5,6), and new bioinformatics indicators, such as tumor-associated macrophages, microRNAs (miRNAs/miRs) and long noncoding RNAs, may hold promise in further optimizing individualized treatment approaches for breast cancer.

miRNAs are a class of non-coding RNAs that are 19-24 nucleotides in length. They function as epigenetic regulators by modulating post-transcriptional gene expression (7,8). The dysregulated expression of miRNAs can have significant effects on various aspects of cancer progression, including metastasis, cell proliferation and chemotherapy resistance. Aberrant expression of specific miRNAs has been associated with the development and recurrence of several types of cancer, including breast, prostate, lung and colon cancer (9). Tumor cells exhibit distinctive miRNA expression profiles, which can lead to a downregulation in the expression levels of numerous tumor suppressor genes or oncogenes during the process of cancer transformation (9,10). Recently, miRNAs have emerged as stable biomarkers in various biological samples, such as tissues, blood, saliva and urine, offering a promising non-invasive approach for diagnostic and prognostic purposes (11,12). Previous studies have shown that miR-96 is significantly upregulated in various types of tumors, including prostate cancer, hepatocellular carcinoma, lung cancer, colorectal cancer, endometrial cancer and breast cancer (13-15). miR-96 exhibits diverse target genes in different types of cancer. For example, in esophageal cancer, one of its target genes is RECK, whereas in hepatocellular carcinoma, it targets EphrinA5 (16). miR-96-5p has been implicated in promoting tumor progression by negatively regulating the tumor suppressor gene FOXO3, which ultimately leads to enhanced cell proliferation (17). However, to date, the biological function of miR-96 in breast cancer is still largely unknown. Therefore, the purpose of the present study was to evaluate the association between

miR-96 and breast cancer, and to explore the potential target genes of miR-96.

TGFβ is a crucial regulator in various biological processes, including cell proliferation, differentiation, apoptosis and immune responses. Proper regulation of TGFβ signaling is essential for maintaining tissue homeostasis and preventing tumorigenesis (18). The TGF-β signaling pathway plays a significant role in promoting the proliferation, invasion and metastasis of tumor cells, as well as aiding in immune evasion by cancer cells (19). Within this pathway, there are inhibitory Smad proteins, namely Smad6 and Smad7, which negatively regulate the activity of the TGF-β signaling pathway (20-22). Smad7, which is one of the key inhibitors of TGF-β signal transduction, negatively regulates the whole pathway through a variety of mechanisms (23,24). miR-96-5p, by targeting Smad7, can exacerbate PPAR-γ/C/EBPα signaling-induced adipogenic differentiation of orbital fibroblasts (25). Another study reported that miR-96 can promote collagen deposition in keloids by targeting Smad7 (26,27).

miR-96, as an oncogene, may be an important regulator of breast cancer cell proliferation, migration and invasion. The present study focused on miR-96 expression in tissue specimens from patients with breast cancer and breast cancer cell lines.

Materials and methods

Human specimens. Breast cancer tissues and paracancerous tissues (~2 cm from tumor tissue) were collected from patients with breast cancer (n=5). The patients were aged between 26 and 43 years (mean ± SD age, 31.12±2.27 years). The numbers of patients with stage I, II and III breast cancer were 2, 2 and 1, respectively, according to the Union for International Cancer Control TNM classification and stage (28). Frozen samples (at -80˚C) were obtained from patients with breast cancer who had undergone tumorectomy or mastectomy after fine needle biopsy diagnosis of breast cancer. Tissues were fixed with 4% paraformaldehyde for 30 min at room temperature and were prepared into 6-μm sections. The thickness was assessed by a professional pathologist. The present study was approved by the Ethics Committee of The People's Hospital of Xinghua City (approval no. JSXHRYLL-YJ-202026; Xinghua, China) and was performed in compliance with The Declaration of Helsinki. Written informed consent was obtained from all participants before surgery.

Reverse transcription-quantitative (RT-q) PCR. A total of five samples of breast cancer tissues and paracancerous tissues were collected. Total RNA was extracted from the tissues using TRIzol® reagent (Invitrogen; Thermo Fisher Scientific, Inc.) and reverse-transcribed into cDNA using a PrimeScript RT Kit (Takara Bio, Inc.) according to the manufacturer's instructions. PCR amplification was performed using the following reaction mixture: 10 μl SYBR Green Mix (Thermo Fisher Scientific, Inc.), 0.4 μl forward primers, 0.4 μl reverse primers, 7.2 μl ddH_2O and 2 μl cDNA template, resulting in a total volume of 20 μl. The amplification conditions were as follows: 94˚C for 10 min, followed by 40 cycles at 94˚C for 20 sec, 55˚C for 20 sec and 72˚C for 20 sec. The relative expression levels of target genes were calculated using the $2^{-\Delta\Delta Cq}$ method (29). GAPDH was used as the internal control for mRNA detection and U6 was used as the internal control for miRNA detection. The primer sequences are listed in Table I.

Western blot analysis. Total protein was extracted from tissues and cells using RIPA cleavage fluid (cat. no. P0013B; Beyotime Institute of Biotechnology), and its concentration was determined using the BCA protein assay kit (QPBCA; MilliporeSigma). The proteins (35 μg) were separated by SDS-PAGE on 8% gels and subsequently transferred to polyvinylidene fluoride membranes. After blocking with 5% BSA (cat. no. BS114; Biosharp Life Sciences) at room temperature for 1 h, the membranes were incubated with specific primary antibodies at 4˚C overnight and then washed three times with PBS-0.1% Tween. The primary antibodies used were Smad7 (cat. no. ab216428; Abcam), AKT (cat. no. ab89402; Abcam), TGF-β (cat. no. ab215715; Abcam), PI3K (cat. no. 20584-1-AP; Proteintech Group, Inc.), BAX (cat. no. ab182733; Abcam), BCL2 (cat. no. ab182858; Abcam), caspase 3 (cat. no. ab13585; Abcam), caspase 9 (cat. no. ab202068; Abcam) and GAPDH (cat. no. 60004-1-Ig; Proteintech Group, Inc.). The primary antibodies were used at a dilution of 1:1,000. The membranes were subsequently incubated with the corresponding horseradish peroxidase-conjugated secondary antibodies (HRP-labeled sheep anti-mouse secondary antibody, cat. no. ZB2305; HRP-labeled sheep anti-rabbit secondary antibody, cat. no. ZB2301; both from OriGene Technologies, Inc.; 1;5,000 dilution) at room temperature for 1 h. The gray values were analyzed by ImageJ 2X software (National Institutes of Health) and the relative expression levels of proteins in each group were calculated.

Cell culture. Breast cancer cell lines (MCF-7, MDA-MB-231, MDA-MB-436 MDA-MB-468 and ZR-75-1) were purchased from Nanjing KeyGen Biotech Co., Ltd. and were cultured in DMEM supplemented with 10% fetal bovine serum (Procell Life Science & Technology Co., Ltd.), 1% L-glutamine, 100 U/ml penicillin and 100 mg/ml streptomycin. The cell lines were authenticated using the short tandem repeat method. The cells were incubated at 37˚C in a humidified atmosphere with 5% CO_2. The cells were negative for mycoplasma. On reaching 80-90% confluence, the cells were transferred to the appropriate plates for subsequent analyses.

Immunohistochemistry. A total of five samples of breast cancer tissues and paracancerous tissues were collected fixed with 4% paraformaldehyde at room temperature for 30 min, dehydrated in a graded ethanol series and then prepared as paraffin-embedded sections (5 μm). Histological slices were blocked with 10% normal goat serum (Beyotime Institute of Biotechnology) at room temperature for 1 h. Subsequently, the sections were incubated overnight at 4˚C with primary antibodies against Smad7 (cat. no. ab216428; Abcam; 1:100), Ki67 (cat. no. ab21700; Abcam), followed by a 1-h incubation at 37˚C with a HRP-conjugated secondary antibody (ready to use; cat. no. PV-9001; OriGene Technologies, Inc.). The nuclei were stained with hematoxylin at room temperature for 5-8 min and the expression levels of Smad7 in tissues were examined by light microscopy.

Table I. Primer sequences.

Name	Primer sequence, 5'-3'
miR-96-5p (human)-F	ACACTCCAGCTGGGTTTGGCACTAGCACATT
URP	TGGTGTCGTGGAGTCG
Smad7 (human)-F	CAACCGCAGCAGTTACCC
Smad7 (human)-R	CGAAAGCCTTGATGGAGA
hsa-mir-96-5p mature sequence	TTTGGCACTAGCACATTTTTGCT
RT reverse primers	CTCAACTGGTGTCGTGGAGTCGGCAATTCAGTTGAGAGCAAAAA
U6 (human)-F	CTCGCTTCGGCAGCACA
U6 (human)-R	AACGCTTCACGAATTTGCGT
GAPDH (human)-F	AGAAGGCTGGGGCTCATTTG
GAPDH (human)-R	AGGGGCCATCCACAGTCTTC

F, forward; R, reverse; miR, microRNA; URP, universal reverse primer.

Dual luciferase assay for verifying the interaction between miR-96 and Smad7. A dual luciferase kit (cat. no. E1910; Promega Corp.) was used to determine the interrelationship between miR-96 and Smad7. The miR-96 binding site in the 3'-UTR of Smad7 was identified using TargetScan version 7.2 (https://www.targetscan.org/vert_72/). Calculations were made by comparing firefly luciferase activity to *Renilla* luciferase activity. The wild-type (WT) Smad7 sequence containing miR-96 binding sites was found on NCBI (https://www.ncbi.nlm.nih.gov/nuccore/KT584248.1) and was used to design a mutant (MUT) sequence (usually complementary to the miR-96 binding site). The sequences were then sent to General Biology (Anhui) Co., Ltd. for direct synthesis into pmirGLO vectors [provided by General Biology (Anhui) Co., Ltd.]. Hsa-miR-96-5p mimics, pmirglo-Smad7 WT-3' UTR and pmirglo-Smad7 MUT-3' UTR were synthesized by Oligobio [provided by General Biology (Anhui) Co., Ltd.] and were transfected into 293T cells (60% confluence; Wuxi Puhe Biomedical Technology Co., Ltd.) using Lipofectamine® 2000 (Invitrogen; Thermo Fisher Scientific, Inc.) according to the manufacturer's instructions. The transfection efficiency was assessed by dual luciferase assay at 48 h post-transfection. The following sequences were used: miR-96-5p mimic, 5'-UUUGGCACAGCACAUUUUUGCUCAAAAAUGUGCUAGUGCCAAAUU-3'; mimic NC, 5'-AGAGGAAACGUGCUAGUGCCAGG-3'.

Knockdown of Smad7 target sequence. For Smad7 knockdown, the plvx-shRNA2-Zsgreen-T2A-puro vector [General Biology (Anhui) Co.,Ltd.] was used. Using a second-generation lentiviral vector system, 293T cells were transfected with a combination of the plasmid containing the target sequence, packaging plasmids (pGag/Pol, pRev), envelope plasmid (pVSV-G) and Lipo8000™ transfection reagent (cat. no. C0533; Beyotime Institute of Biotechnology); the plasmid ratio for the target gene plasmid, packaging plasmids and envelope plasmid was 1:4:3, corresponding to 2.5, 10 and 7.5 μg, respectively. Transfection was carried out at 37˚C in a 5% CO_2 incubator for 6 h. After 6 h, the medium was replaced with complete culture medium and the cells were cultured for 72 h. Subsequently, the cell supernatant enriched with lentiviral particles was collected by centrifugation at 3,000 x g for 4 min at 4˚C. The supernatant was filter through a 0.45-μm filter, and the lentiviral particles were concentrated by ultracentrifugation at 32,000 x g for 2 h at 4˚C. The concentrated viral suspension was then aliquoted into labeled tubes and stored at -80˚C. The day before infection, 4x10^3 MDA-MB-231 cells were seeded into each well of a 96-well plate. When the MDA-MB-231 cell density reached 50%, the virus was directly added to the complete culture medium at a multiplicity of infection of 100. The cells were incubated with the virus for 72 h at 37˚C. To create a stable cell line, transduced cells were selected using puromycin solution (cat. no. BL528A; Biosharp) at a concentration of 2.5 μg/ml. The sequences were as follows: shRNANC, 5'-GGTATAGCCAGCTAACTAGAA-3'; shRNA-Smad7-1, 5'-GCTTTCAGATTCCCAACTTCT-3'; shRNA-Smad7-2, 5'-GGTTTCTCCATCAAGGCTTTC-3'; shRNA-Smad7-3, 5'-GCTCCCATCCTGTGTGTTAAG-3'. The data were analyzed by ABI Prism 7500 SDS software (Applied Biosystems; Thermo Fisher Scientific, Inc.). RT-qPCR assays were conducted to verify the expression levels of target genes following transfection.

Functional analysis of miR-96-5p and its interaction with Smad7. MDA-MB-231 and MDA-MB-468 cells (1x10^5/well) were seeded into a 24-well plate and incubated under standard conditions in complete medium. The transfection reagents were prepared by mixing miR-96-5p negative control (NC), miR-96-5p mimics + overexpression-negative control (OE-NC; empty pcDNA3.1-EGFP plasmid), miR-96-5p NC + overexpression-Smad7 (OE-Smad7) and miR-96-5p inhibitor [all supplied by General Biology (Anhui) Co., Ltd.] with Lipo8000 to form the transfection complex. In addition, cells that had already been virally infected with shRNA-Smad7 were subsequently transfected with the miR-96-5p inhibitor. This step was based on the protocol for Lipo8000 transfection reagent, using 500 ng plasmid/well in a 24-well plate, with an RNA concentration of 20 pmol. The transfection complex was added to the cells and incubated under standard conditions for 4-6 h. Subsequently, the supernatant was removed and the cells were incubated in complete medium for another

48 h before being collected for further analysis. The following sequences were used: miR-96-5p mimics, 5'-UUUGGCACA GCACAUUUUUGCUCAAAAAUGUGCUAGUGCCAA AUU-3'; miR-96-5p inhibitor NC, 5'-CAGUACUUUUGU GUAGUACAA-3'; miR-96-5p mimic NC, 5'-AGAGGAAAC GUGCUAGUGCCAGG-3'; miR-96-5p inhibitor, 5'-AGC AAAAAUGUGCUAGUGCCAAA-3'.

Transwell assays for cell invasion and migration. First, 100 μl serum-free medium was added to the upper chamber of a Transwell system (pore size, 8 μm; cat. no. 3422; Corning, Inc.), while 600 μl complete medium was added to the lower chamber. Subsequently, transfected MDA-MB-231 and MDA-MB-468 cells were added to the upper chamber at a density of $4x10^4$/well and were cultured 24 h 37˚C. Next, the cells were fixed with pre-cooled 4% paraformaldehyde at room temperature for 30 min and stained with 0.5% crystal violet at room temperature for 10 min. Finally, the polycarbonate film was obtained from the upper chamber, sealed and observed under a light microscope. In addition, the upper chamber of the Transwell system was coated with Matrigel at 37˚C for 30 min for the cell invasion assay, and the rest of the steps were the same as those performed for the cell migration assay.

Determination of cell adhesion. First, 100 μl coating solution in the Cell Adhesion Assay Kit (cat. no. BB-48120; Bstbio) was added to a 96-well plate at 2-8˚C overnight. The coating fluid was removed and the culture vessels were dried. The washing solution (PBS) was used to wash the vessels 1-3 times. Transfected MDA-MB-231 and MDA-MB-468 cells were digested with trypsin and collected, washed with PBS and then suspended in the corresponding medium to prepare a cell suspension. Cell suspensions containing $5x10^4$ cells/well were incubated in a 96-well plate with three multiple wells. To each well of the 96-well plate 10 μl cell staining solution B was added and incubated at 37˚C for 2 h. The $OD_{450\ nm}$ values of the sample wells were measured.

Nude mouse tumorigenicity model. Nude mice were obtained from Changzhou Cavens Experimental Animal Co., Ltd. All experiments were approved by the Institutional Animal Care and Use Committee of the Affiliated Hospital of Yangzhou University (this hospital has a partnership with Yangzhou University; approval no. JSXHRYLL-YJ-202026; Jiangsu, China). All animal experiments were performed in compliance with animal ethics (30) and EU Directive 2010/63/EU (31). A total of 9 specific pathogen-free-rated healthy male nude mice (age, 4-6 weeks; weighing, 20 g), housed at 40-60% humidity and ~25˚C, under a 12-h light/dark environment. The mice were maintained in a clean environment, avoiding bright light and noise, and were given free access to food and water. On an ultra-clean table, the skin at the injection site of the nude mice was disinfected using 75% alcohol. Subsequently, 100 μl 1X PBS containing $5x10^6$ MDA-MB-231 cells was injected into the armpits of the nude mice according to their respective groups. For cell inoculation, the needle was inserted under the skin, about 1 cm deep, in order to minimize the overflow of the cell suspension from the eye of the needle after the injection. This was to prevent liquid leakage, sterilize the skin and facilitate observation of tumor formation. Tumor size in the nude mice was measured every 3 days. The longest and shortest tumor diameters were measured using vernier calipers and the tumor volume (V, in mm^3) was calculated using the formula $V=(AB^2)/2$, where A and B represent the longest and shortest tumor diameters, respectively. The tumor size of nude mice was measured every 3 days and recorded. When tumor mass was ~100 mm^3, each mouse was injected with 100 μl 20 nmol miR-96-5p mimics NC, miR-96-5p mimics or miR-96-5p inhibitor for 3 consecutive days. The following sequences were used: miR-96-5p mimic: 5'-UUUGGCACAGCACAUUUU UGCUCAAAAAUGUGCUAGUGCCAAAUU-3', miR-96-5p inhibitor: 5'-AGCAAAAAUGUGCUAGUGCCAAA-3' and mimics NC: 5'-AGAGGAAACGUGCUAGUGCCAGG-3'. The mice in the control group were intratumorally injected with normal saline. After 3 weeks of treatment, the nude mice were sacrificed for tumor collection. The method used was isoflurane inhalation at a concentration of 5%.

Cell cycle analysis. For cell cycle analysis, the transfected MDA-MB-231 and MDA-MB-468 cells were seeded in 6-well plates at a density of $1x10^6$ cells per well. Then, the cells were harvested, fixed with 80% ethanol at 4˚C overnight, then treated with 50 μg/ml PI and 100 μl RNase (100 μg/ml) for 30 min at room temperature in the dark. The fixed/stained cells were analyzed using a FACSCalibur flow cytometer (BD Biosciences) and ModFit LT 5.0 (Verity Software House).

Statistical analysis. Statistical analysis was conducted with GraphPad Prism 5.0 software (Dotmatics). Data are presented as the mean ± SD; *in vitro* experiments n=3, clinical experiments n=5. For data that followed a normal distribution, Student's unpaired t-test was used to compare the difference between two groups. For multi-group comparisons of variables, one-way ANOVA was used with the Tukey's post hoc test. $P<0.05$ was considered to indicate a statistically significant difference.

Results

Expression levels of miR-96 and Smad7 are significantly increased and decreased in breast cancer tissues, respectively. The present study explored the differences in miR-96 and Smad7 expression levels between breast cancer tissues and adjacent tissues, and verified the roles of miR-96-5p and Smad7 in breast cancer. Breast cancer and adjacent non-tumor tissues were collected from five patients with breast cancer, and the differences in miR-96 and Smad7 expression levels between the tissues were detected by RT-qPCR. As shown in Fig. 1A, the expression levels of miR-96-5p were significantly higher in breast cancer tissues than in adjacent tissues, while the expression levels of Smad7 were significantly lower in breast cancer tissues than in adjacent tissues. Western blot analysis and immunohistochemical staining revealed that the expression levels of Smad7 were markedly reduced in breast cancer tissues compared with those in adjacent tissues (Fig. 1B and C). Expression of the target protein appears as brown staining.

miR-96 can bind Smad7. To investigate the relationship between miR-96 and Smad7, miR-96-5p mimics were first synthesized, and WT and MUT plasmids for Smad7-3'UTR

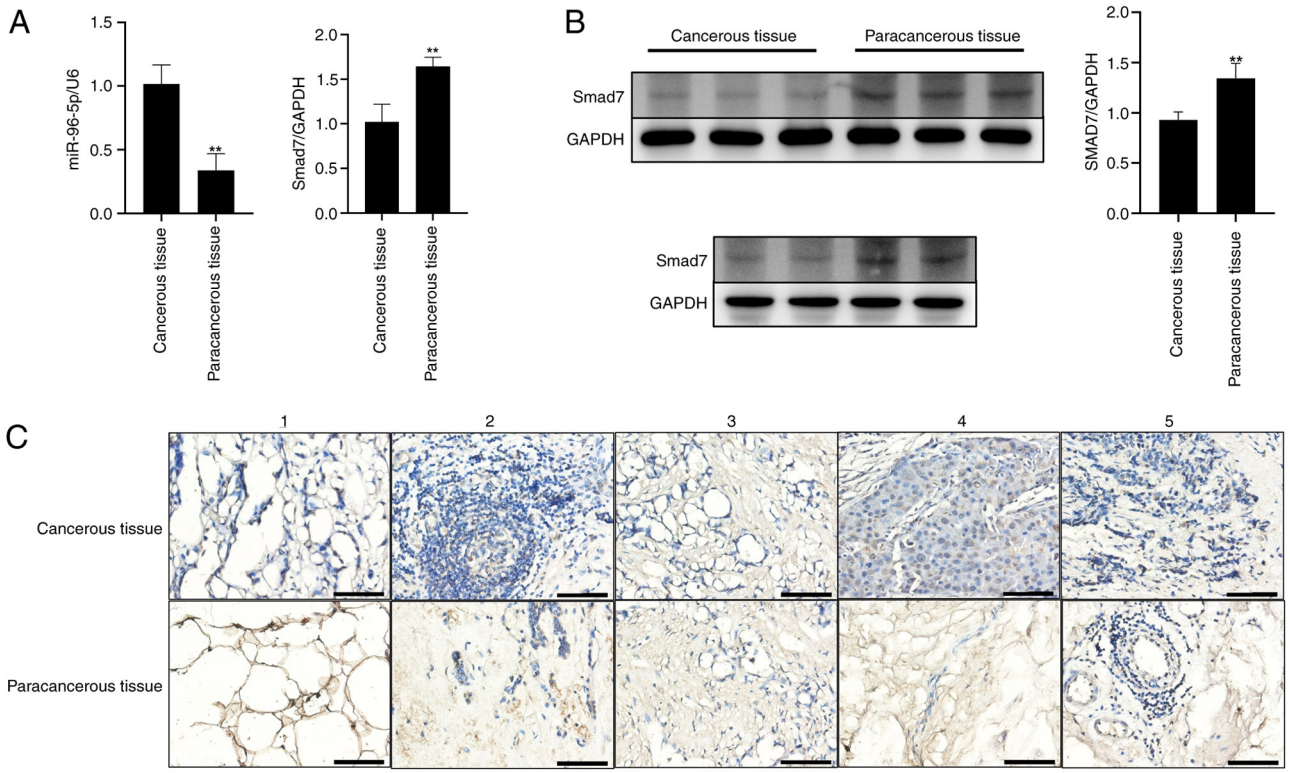

Figure 1. Expression levels of miR-96 and Smad7 are significantly increased and decreased in breast cancer tissues, respectively. (A) Reverse transcription-quantitative PCR analysis of the relative expression levels of miR-96 and Smad7 in breast cancer tissues and matched adjacent noncancerous tissues. (B) Western blot analysis of the relative expression levels of Smad7 in breast cancer tissues and matched adjacent noncancerous tissues. Bar plot showing the grayscale data of Smad7 and GAPDH. (C) Expression of Smad7 in breast cancer and paracancerous tissues were assessed using an anti-Smad7 antibody. **P<0.01 vs. Cancerous tissue. miR, microRNA.

constructed. Subsequently, 293T cells were transfected and changes in activity were measured using a dual luciferase kit. The experimental results demonstrated that, in comparison to the NC group, co-transfection of 293T cells with the WT Smad7 vector and miR-96-5p mimics led to a significant reduction in luciferase activity (Fig. 2). However, when the predicted binding site (g.51537A>G) was mutated, there was no significant difference in luciferase activity compared with the NC group (Fig. 2). These findings indicated that miR-96-5p has the ability to target and bind to Smad7.

Among the five breast cancer cell lines, miR-96 expression is highest and Smad7 expression is lowest in MDA-MB-231 cells. To determine the expression levels of miR-96 and Smad7 in breast cancer, RT-qPCR was conducted to detect their mRNA expression levels in different breast cancer cell lines, including MCF-7, MDA-MB-231, MDA-MB-436, MDA-MB-468 and ZR-75-1. The experimental results showed that miR-96 exhibited the highest expression in MDA-MB-231 cells. Conversely, the expression levels of Smad7 were found to be the lowest in MDA-MB-231 cells (Fig. 3A and B). Subsequently, western blotting was conducted to assess the expression levels of Smad7 in different breast cancer cell lines. The findings demonstrated that Smad7 expression was the lowest in MDA-MB-231 cells (Fig. 3C and D).

miR-96 reduces the expression of Smad7 in MDA-MB-231 and MDA-MB-468 cells. The present study designed and

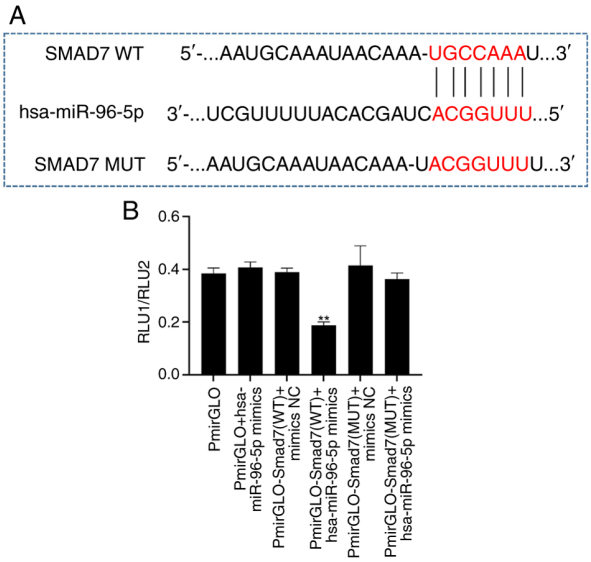

Figure 2. Validation of target genes by dual luciferase assay. (A) miR-96 binding site in the 3'-UTR of Smad7. (B) Targeted binding of miR-96 and SMAD7 was verified by dual luciferase assay. **P<0.01 vs. NC. miR, microRNA; NC, negative control; WT, wild type; MUT, mutant; RLU, relative light unit.

synthesized three shRNA-Smad7 plasmids. All of the plasmids were transfected into the MDA-MB-231 breast cancer cell line. After transfection, RNA was extracted from each group of cells

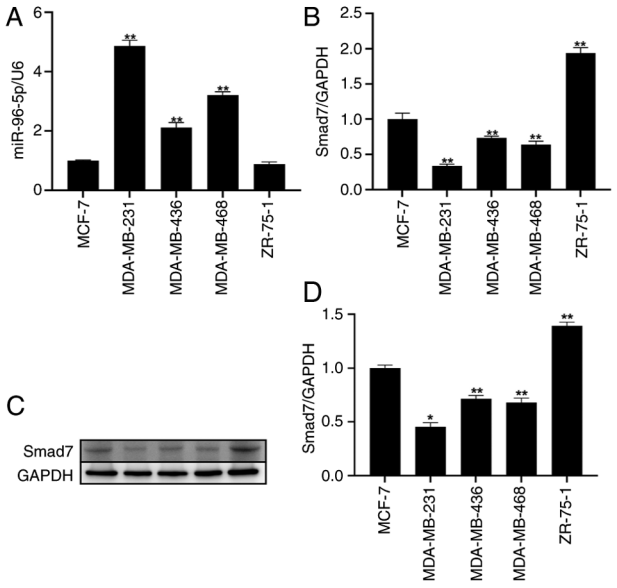

Figure 3. Expression levels of miR-96 and Smad7 are higher and lower in MDA-MB231 cells than in other breast cancer cells, respectively. Comparison of (A) miR-96 and (B) Smad7 expression levels in different breast cancer cell lines by RT-qPCR assay. (C) Western blotting analysis of Smad7. (D) Comparison of Smad7 expression levels in different breast cancer cell lines by western blotting. *P<0.05, **P<0.01 vs. MCF-7. miR, microRNA; RT-qPCR, reverse transcription-quantitative PCR.

and was reverse-transcribed into cDNA for RT-qPCR analysis. The experimental results, as shown in Fig. S1A, indicated that different shRNAs had distinct knockdown effects on Smad7 mRNA expression levels. Among them, shRNA-Smad7-2 exhibited the most marked knockdown effect.

As shown in Fig. S2, compared with in the mimics NC group, miR-96-5p expression was increased after MDA-MB-231 and MDA-MB-468 cells were transfected with miR-96-5p mimics. Compared with in the inhibitor NC group, the expression levels of miR-96-5p were decreased post-transfection with the miR-96-5p inhibitor. As shown in Fig. S3, compared with in the OE NC group, an increase in Smad7 expression was detected in MDA-MB-231 and MDA-MB-468 cells transfected with OE Smad7, and compared with in the shRNA NC group, a decrease in Smad7 expression was detected after transfection with shRNA Smad7. These findings indicated that transfection was successful. Since the expression levels of miR-96-5p in the mimics NC and inhibitor NC groups were consistent, both were subsequently represented by a mimics NC.

RT-qPCR was used to verify the expression levels of target genes in MDA-MB-231 and MDA-MB-468 cells following transfection with miR-96-5p mimics and shRNA-Smad7 plasmids. Total RNA was extracted and reverse-transcribed into cDNA. RT-qPCR and western blotting results showed that, compared with miR-96-5p NC group, the expression levels of miR-96-5p and Smad7 were significantly increased and decreased post-transfection with miR-96-5p mimics, respectively (Fig. 4A-D). Furthermore, compared with in cells transfected with miR-96-5p mimics, the expression levels of miR-96-5p and Smad7 were significantly decreased and increased, respectively, in response to overexpression of Smad7. Compared with in the miR-96-5p NC group, post-transfection with the miR-96-5p inhibitor, the expression levels of miR-96-5p were significantly decreased, whereas those of Smad7 were significantly increased. Furthermore, compared with in cells transfected with miR-96-5p inhibitor, the expression levels of miR-96-5p and Smad7 were significantly increased and decreased, respectively, following transfection with shRNA-Smad7.

miR-96 promotes the migration and invasion of breast cancer cells by inhibiting the expression of Smad7. Following transfection with miR-96-5p mimics + OE-Smad7, there was a reduction in the number of cells in the G_0/G_1 phase compared with control group (Fig. S1B). Compared with control group, transfection with the miR-96-5p inhibitor resulted in an increase in cells in the G_0/G_1 phase. In addition, compared with in cells transfected with the miR-96-5p inhibitor, miR-96-5p inhibitor + shRNA-Smad7 led to a decrease in cells in the G_0/G_1 phase; this decrease was significant in MDA-MB-468 cells. Compared with in the control group, transfection with miR-96-5p mimics + OE Smad7 could increase the number of cells in the G_2/M phase. Transfection with miR-96-5p inhibitor + shRNA-Smad7 significantly increased the number of cells in the G_2/M phase, compared with in the miR-96-5p inhibitor group. Furthermore, compared with control group, the number of cells in S phase decreased after transfection with the miR-96-5p inhibitor.

In comparison with the control group, there were no significant differences in cell adhesion ability observed in the miR-96-5p NC group (Fig. 5A). However, compared with in the control group, cell adhesion ability was significantly enhanced in the miR-96-5p mimics + OE-NC group. Conversely, the cell adhesion ability was significantly decreased in the miR-96-5p inhibitor group. When comparing the miR-96-5p mimics + OE-NC group with the miR-96-5p mimics + OE-Smad7 group, the cell adhesion ability was significantly reduced. Additionally, the cell adhesion ability of the miR-96-5p inhibitor + shRNA-Smad7 group was significantly enhanced compared with the miR-96-5p inhibitor group. Furthermore, a Transwell assay was performed to assess the migration and invasion of cells, as shown in Fig. 5B and C. Compared with in the control group, there were no significant differences in the migration and invasion of cells observed in the miR-96-5p NC group. However, compared with in the control group, the migration and invasion of cells were significantly enhanced in the miR-96-5p mimics + OE-NC group. Conversely, the invasion and migration of cells were significantly reduced in the miR-96-5p inhibitor group. When comparing the miR-96-5p mimics + OE-NC group with the miR-96-5p mimics + OE-Smad7 group, the migration and invasion of cells were significantly reduced. In addition, the migration and invasion of the miR-96-5p inhibitor + shRNA-Smad7 group were significantly enhanced compared with in the miR-96-5p inhibitor group.

miR-96 can promote activation of the TGF-β signaling pathway. As shown in Fig. 6, the transfection of MDA-MB-231 cells with miR-96-5p mimics significantly increased the expression levels of AKT, TGF-β, PI3K and Bcl-2, while significantly decreasing the expression levels of Bax, caspase 3 and caspase 9, compared with those in the control group. Compared with in the miR-96-5p mimics + OE NC group,

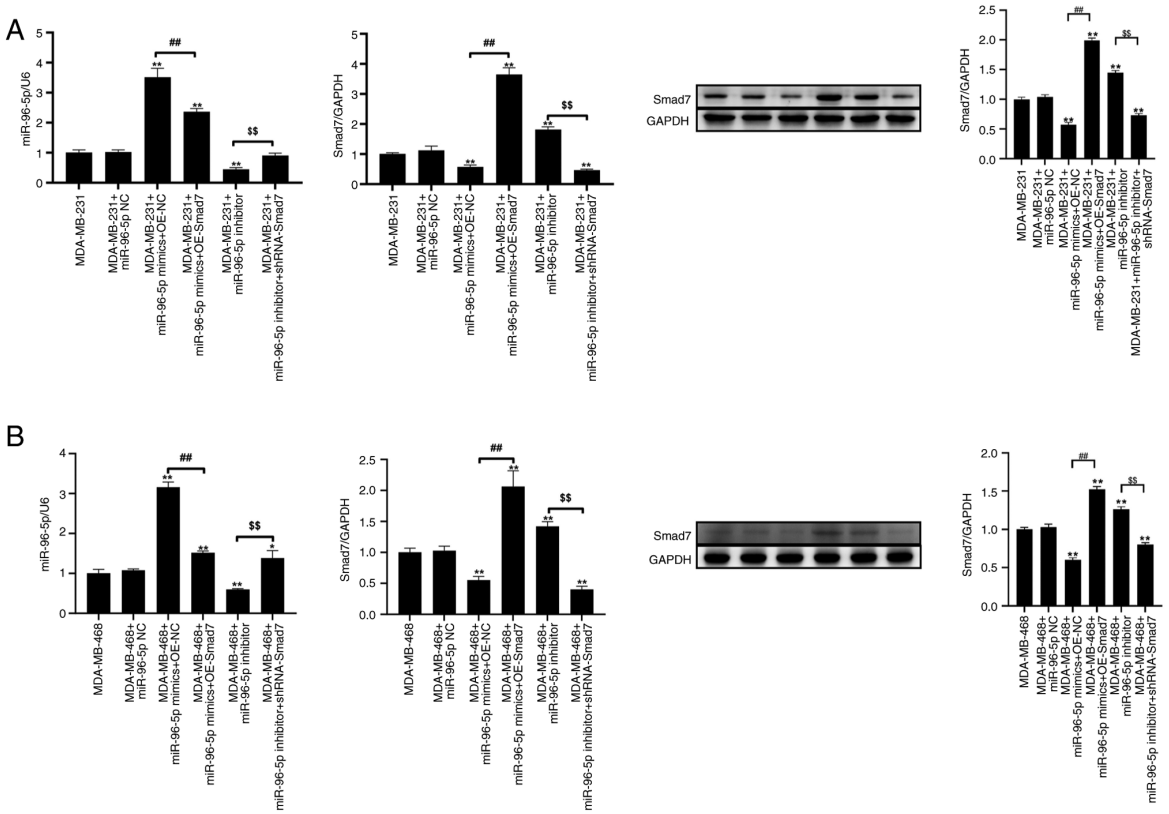

Figure 4. miR-96 inhibits the expression of Smad7 in MDA-MB-231 and MDA-MB-468 cells. (A) Expression levels of target genes following transfection with miR-96-5p mimics and shRNA-Smad7 in MDA-MB-231 cells. **P<0.01 vs. MDA-MB-231; $^{\#\#}$P<0.01 vs. MDA-MB-231 + miR-96-5p mimics + OE-NC; $^{\$\$}$P<0.01 vs. MDA-MB-231 + miR-96-5p inhibitor. (B) Expression levels of target genes following transfection with miR-96-5p mimics and shRNA-Smad7 in MDA-MB-468 cells. *P<0.05, **P<0.01 vs. MDA-MB-468; $^{\#\#}$P<0.01 vs. MDA-MB-468 + miR-96-5p mimics + OE-NC; $^{\$\$}$P<0.01 vs. MDA-MB-468 + miR-96-5p inhibitor. miR, microRNA; OE, overexpression; NC, negative control.

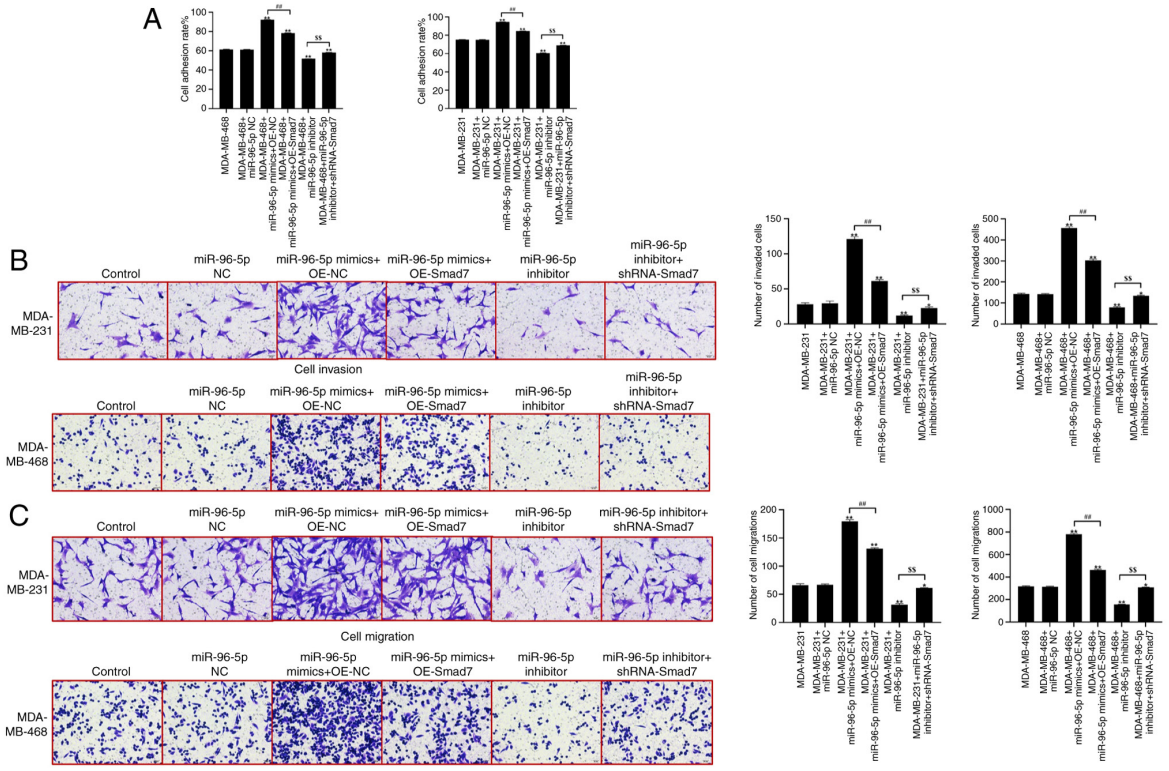

Figure 5. miR-96 promotes the migration and invasion of breast cancer cells by inhibiting Smad7 expression. (A) Determination of cell adhesion. Cell (B) invasion and (C) migration was assessed in MDA-MB-231 and MDA-MB-468 cells by Transwell assay. **P<0.01 vs. Control; $^{\#\#}$P<0.01 vs. miR-96-5p mimics + OE Smad7; $^{\$\$}$P<0.01 vs. miR-96-5p inhibitor + shRNA-Smad7. miR, microRNA; OE, overexpression; NC, negative control.

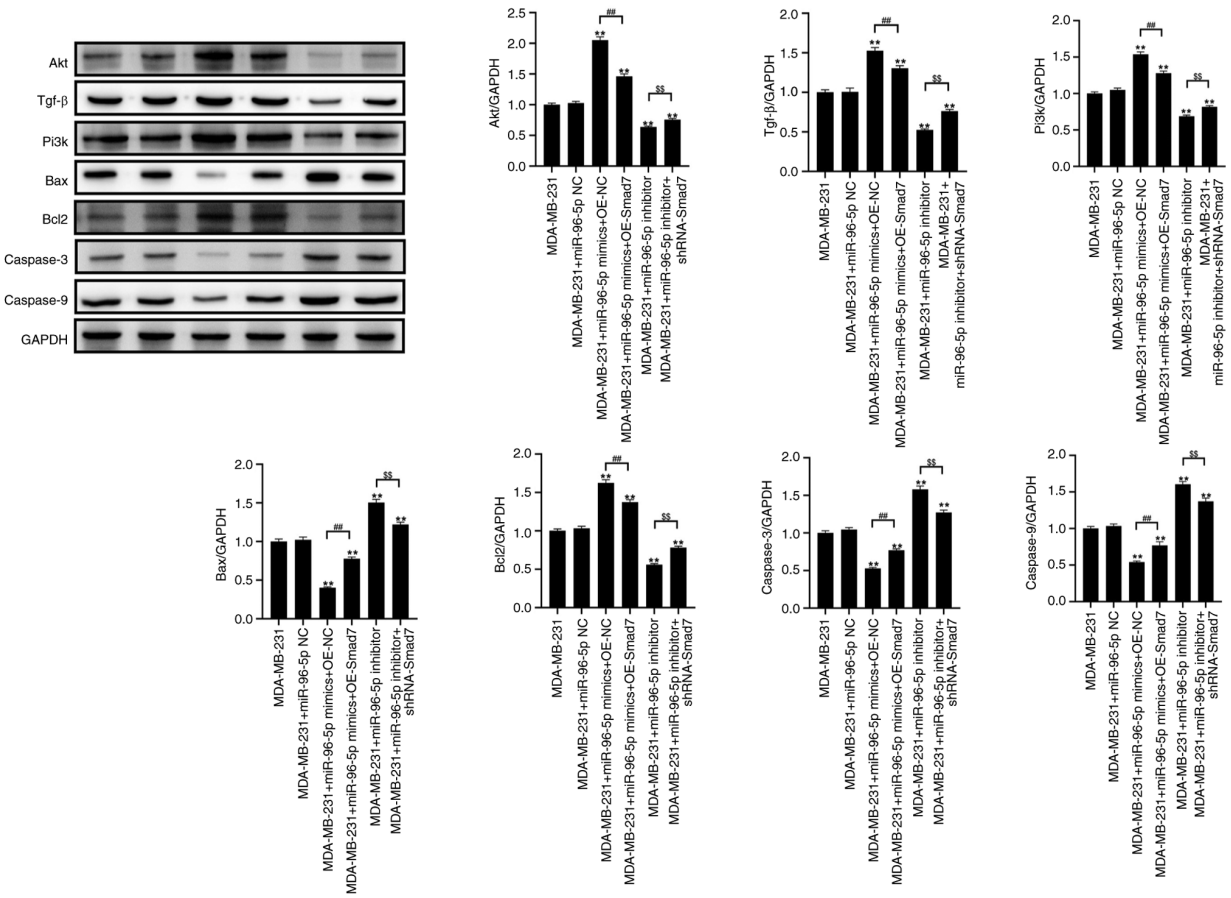

Figure 6. Western blotting of proteins involved in tumor-related signaling. **P<0.01 vs. Control; $^{\#\#}$P<0.01 vs. MDA-MB-231+miR-96-5p NC; $^{\$\$}$P<0.01 vs. MDA-MB-231+miR-96-5p inhibitor. miR, microRNA; sh, short hairpin; OE, overexpression; NC, negative control.

transfection with miR-96-5p mimics + OE Smad7 led to a significant decrease in the expression levels of TGF-β, PI3K and Bcl-2, and an increase in the expression levels of Bax, caspase 3 and caspase 9. Compared with in the control group, after transfection with the miR-96-5p inhibitor, the expression levels of TGF-β, PI3K and Bcl-2 were significantly decreased, whereas those of Bax, caspase 3 and caspase 9 were significantly increased. Furthermore, transfection with miR-96-5p inhibitor + shRNA-Smad7 resulted in increased expression levels of TGF-β, PI3K and Bcl-2, while the expression levels of Bax, caspase 3 and caspase 9 were significantly decreased compared with those in the miR-96-5p inhibitor group.

miR-96 can promote the proliferation of breast cancer cells in a nude mouse tumorigenicity model. To explore the effects of miR-96 on the proliferation of breast cancer *in vivo*, the present study established a nude mouse tumorigenicity model. The results demonstrated that, in comparison with the NC group, the tumor size in mice treated with miR-96-5p mimics was significantly increased; however, after treatment with the miR-96-5p inhibitor, the tumor size decreased (Fig. 7A). The RT-qPCR results indicated that the expression levels of miR-96-5p in tumor tissues were significantly increased and reduced following treatment with miR-96-5p mimics and the miR-96-5p inhibitor, compared with NC group, respectively. Western blot analysis revealed that the expression levels of Smad7 in tumor tissues were significantly decreased and increased after treatment with miR-96-5p mimics and the miR-96-5p inhibitor, respectively (Fig. 7B). Next, the present study investigated the expression of the tumor-related gene caspase 3. The results of histological staining demonstrated that the expression levels of caspase 3 were decreased and increased after treatment with miR-96-5p mimics and the miR-96-5p inhibitor, respectively. Compared with in the NC group, Ki67 expression was increased in the miR-96-5p mimics group and decreased in the miR-96-5p inhibitor group (Fig. 7C).

Discussion

Breast cancer accounts for ~15% of cancer-related deaths in women worldwide. Although surgical treatment can effectively remove malignant tumors, it can seriously damage the physical and mental health of patients (32,33). Based on molecular and histological evidence, breast cancers can be divided into three categories: Breast cancers expressing hormone receptors (estrogen receptor or progesterone receptor), breast cancers expressing human epidermal receptor 2 and triple-negative breast cancers (34). Single-stranded miRNA molecules contain ~22 nucleotides and function as a central dogma of molecular biology by inhibiting the process of translation. It has been shown that any alteration in miRNA sequences, especially single-nucleotide polymorphisms, can lead to an increased risk of breast cancer (35).

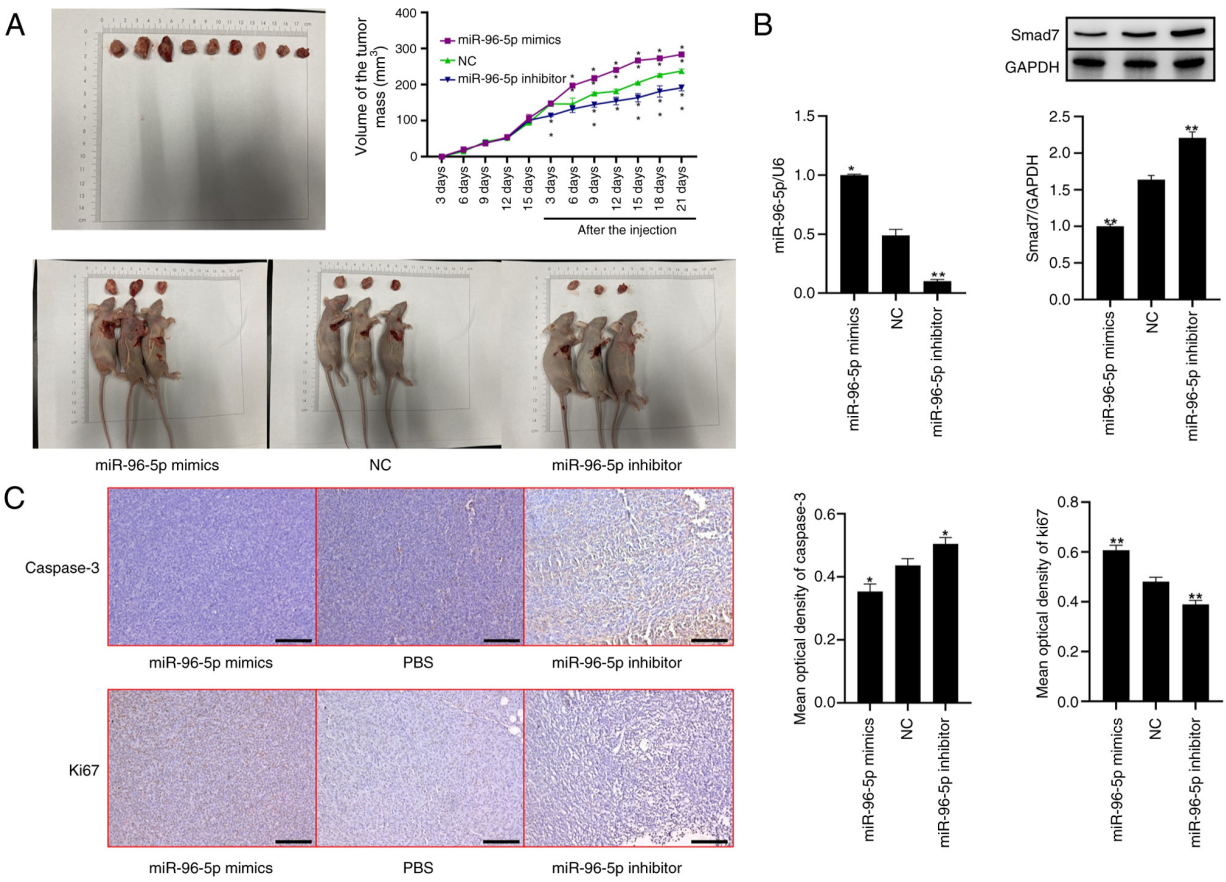

Figure 7. Nude mouse tumorigenicity model. (A) Nude mouse tumorigenicity model was used to explore the role of miR-96 *in vivo*. (B) RT-qPCR and western blotting were performed to detect the expression levels of miR-96 and Smad7 *in vivo*. (C) Immunohistochemical staining was conducted to examine the role of miR-96 *in vivo*. *P<0.05, **P<0.01 vs. NC. miR, microRNA; NC, negative control.

miRNAs play important roles in several biological functions, such as regulation of cell development, differentiation, apoptosis and metastasis (36). In the pathological state, miRNAs can function as both tumor suppressors and tumor promoters, and they play a significant role in the occurrence and development of tumors (37). It has also been reported that miR-96-5p promotes the proliferation and migration of ovarian cancer by inhibiting caveolin 1 (CAV1), which is a 21-24 kDa protein that functions as the primary structural protein component of caveolae. Through interactions with other protein and nonprotein components, CAV1 aids in vesicular trafficking and signal transduction (38). The present study found that the expression levels of miR-96-5p in breast cancer were significantly increased, suggesting that miR-96-5p overexpression may lead to the development of breast cancer.

Polypeptides of the TGF-β family exert their functions by interacting with two related, functionally distinct transmembrane receptor kinases, first interacting with the type II receptor (TβR II) and subsequently with the type I receptor (TβR I). First, TβR II autophosphorylates its amino acid residue, and then interacts with and activates TβR I. Next, the activated TβR I phosphorylates the downstream signaling molecules, Smad2 and Smad3. Then, Smad4 trimer complexes enter the nucleus. With the assistance of DNA-binding cofactors, the trimer complexes bind to the Smad-binding element region on DNA to induce transcription, and ultimately regulate cell proliferation, differentiation and apoptosis (39,40). Smad7 is a negative modulator of the TGF-β signal transduction pathway (41). Smad7 forms a stable complex with TβR I under ligand stimulation and inhibits the recruitment of R-Smads (42). Upon activation, several E3 ubiquitin ligases, such as SmurF1/2 and NEDD4-2 and WWP1/Tiul1, can be recruited, resulting in the polyubiquitination and degradation of TβR I.

The present study revealed that the expression levels of Smad7 were decreased in breast cancer tissues, and RT-qPCR was used to verify the expression levels of target genes following transfection with miR-96-5p mimics and shRNA-Smad7. Following transfection of MDA-MB-231 cells with miR-96-5p mimics and shRNA-Smad7, the expression levels of miR-96-5p were significantly increased, whereas those of Smad7 were significantly decreased. By contrast, the expression levels of miR-96-5p and Smad7 were significantly decreased and increased, respectively, following overexpression of Smad7. After transfection with the miR-96-5p inhibitor, the expression levels of miR-96-5p were significantly decreased, whereas those of Smad7 were significantly increased. By contrast, the expression levels of miR-96-5p and Smad7 were significantly increased and decreased, respectively, following transfection with shRNA-Smad7. Altogether, the results suggested that miR-96 is highly expressed in breast cancer tissues. Notably, miR-96 can inhibit the expression of Smad7, which in turn may activate TGF-β signaling pathway. According to the results of previous studies, lncRNA-Smad has anti-apoptotic functions.

In response to TGF-β stimulation in the mouse breast cancer cell line JygMC(A), lncRNA-Smad7 manifested a discernible anti-apoptotic effect (43). Furthermore, the transcription of the antisense strand upstream of the Smad7 gene produces a lncRNA-Smad7, which interacts with the inhibitor of TGF-β signaling, BMP2 (44,45), thereby selectively preventing TGF-β-induced apoptosis in cancer cells (46).

Tumor invasion and migration are critical factors in breast cancer progression. Growing evidence has suggested that Smad7 can interfere with the carcinogenic effects of TGF-β and other cancer-promoting pathways, thereby inhibiting tumor progression (47,48). TGF-β signal transduction is involved in the epithelial-mesenchymal transformation pathway, which can promote tumor invasion and migration. The present study demonstrated that the expression levels of miR-96 in breast cancer tissues were significantly higher than those in adjacent tissues. Overexpression of miR-96 could promote the migration of breast cancer cells by downregulating Smad7 expression, which is consistent with the findings of a previous study (49). However, miR-96 inhibition could promote the expression of Smad7 and activate the TGF-β signaling pathway, which is in agreement with previous findings (50). These data imply that miR-96 may serve as a prognostic marker for breast cancer.

The present study aimed to examine how miR-96 affects the migration and proliferation of breast cancer cells. Overexpression of miR-96 could promote the proliferation, migration and invasion of breast cancer cells by inhibiting the expression of Smad7; therefore, miR-96 may promote breast cancer via blocking Smad7. In addition, the present study found that silencing Smad7 by RNA interference was able to mimic the carcinogenic effect of miR-96. However, further studies are needed to investigate the relationship between genes and proteins associated with breast cancer by combining more techniques, such as co-immunoprecipitation and chromatin immunoprecipitation. In conclusion, the present study may provide a basic experimental and theoretical basis for the clinical diagnosis of breast cancer.

Acknowledgements

Not applicable.

Funding

The present study was supported by the Science and Technology Support Program Social Development (Instructive) Project of Taizhou (grant no. 2020-30).

Availability of data and materials

The datasets used and/or analyzed during the current study are available from the corresponding author on reasonable request.

Authors' contributions

XZ and YZ conceived and designed the study. Experiments were performed by XZ, LC and XH. RY, QY and YZ analyzed and interpretation of data. XZ and YZ wrote the manuscript. YZ and XZ confirm the authenticity of all the raw data. All authors read and approved the final version of the manuscript.

Ethics approval and consent to participate

The present study was approved by the ethics committee of The People's Hospital of Xinghua City (Jiangsu, China; approval number: JSXHRYLL-YJ-202026) and was performed in compliance with The Declaration of Helsinki. Written informed consent was obtained from all participants before surgery. Animal experiments were approved by the Institutional Animal Care and Use Committee of the Affiliated Hospital of Yangzhou University (approval no. JSXHRYLL-YJ-202026; Jiangsu, China).

Patient consent for publication

Not applicable.

Competing interests

The authors declare that they have no competing interests.

References

1. Aini S, Bolati S, Ding W, Liu S, Su P, Aili S, Naman Y and Xuekelaiti K: LncRNA LncRNA SNHG10 suppresses the development of doxorubicin resistance by downregulating miR-302b in triple-negative breast cancer. Bioengineered 13: 11430-11439, 2022.
2. Alves MT, da Conceição IMCA, de Oliveira AN, Oliveira HHM, Soares CE, de Paula Sabino A, Silva LM, Simões R, Luizon MR and Gomes KB: microRNA miR-133a as a biomarker for Doxorubicin-Induced cardiotoxicity in women with breast cancer: A signaling pathway investigation. Cardiovasc Toxicol 22: 655-662, 2022.
3. Azadeh M, Salehzadeh A, Ghaedi K and Talesh Sasani S: NEAT1 can be a diagnostic biomarker in the breast cancer and gastric cancer patients by targeting XIST, hsa-miR-612 and MTRNR2L8: Integrated RNA targetome interaction and experimental expression analysis. Genes Environ 44: 16, 2022.
4. Cantini L, Bertoli G, Cava C, Dubois T, Zinovyev A, Caselle M, Castiglioni I, Barillot E and Martignetti L: Identification of microRNA clusters cooperatively acting on epithelial to mesenchymal transition in triple negative breast cancer. Nucleic Acids Res 47: 2205-2215, 2019.
5. Chen WH, Luo GF, Sohn YS, Nechushtai R and Willner I: miRNA-specific unlocking of drug-loaded metal-organic framework nanoparticles: Targeted cytotoxicity toward cancer cells. Small 15: e1900935, 2019.
6. Di Cosimo S, Appierto V, Pizzamiglio S, Tiberio P, Iorio MV, Hilbers F, de Azambuja E, de la Peña L, Izquierdo M, Huober J, *et al*: Plasma miRNA levels for predicting therapeutic response to neoadjuvant treatment in HER2-positive breast cancer: Results from the NeoALTTO trial. Clin Cancer Res 25: 3887-3895, 2019.
7. Hajivalili M, Baghaei K, Mosaffa N, Niknam B and Amani D: Engineering tumor-derived small extra cellular vesicles to encapsulate miR-34a, effectively inhibits 4T1 cell proliferation, migration and gene expression. Med Oncol 39: 93, 2022.
8. He C, Wang M, Sun X, Zhu Y, Zhou X, Xiao S, Zhang Q, Liu F, Yu Y, Liang H and Zou G: Integrating PDA microtube waveguide system with heterogeneous CHA amplification strategy towards superior sensitive detection of miRNA. Biosens Bioelectron 129: 50-57, 2019.
9. Huang R, Yang Z, Liu Q, Liu B, Ding X and Wang Z: CircRNA DDX21 acts as a prognostic factor and sponge of miR-1264/QKI axis to weaken the progression of triple-negative breast cancer. Clin Transl Med 12: e768, 2022.
10. Huang W, Wu X, Xiang S, Qiao M, Cen X, Pan X, Huang X and Zhao Z: Regulatory mechanism of miR-20a-5p expression in cancer. Cell Death Discov 8: 262, 2022.
11. Iranparast S, Tahmasebi-Birgani M, Motamedfar A, Amari A and Ghafourian M: Altered expression levels of MicroRNA-155 and SOCS-1 in peripheral blood mononuclear cells of newly diagnosed breast cancer patients. Iran J Allergy Asthma Immunol 21: 12-19, 2022.

12. Jahangiri L and Ishola T: Dormancy in breast cancer, the role of autophagy, lncRNAs, miRNAs and exosomes. Int J Mol Sci 23: 5271, 2022.
13. Lee JU, Kim WH, Lee HS, Park KH and Sim SJ: Quantitative and specific detection of exosomal miRNAs for accurate diagnosis of breast cancer using a Surface-Enhanced raman scattering sensor based on Plasmonic Head-Flocked gold Nanopillars. Small 15: e1804968, 2019.
14. Li J, Gao X, Zhang Z, Lai Y, Lin X, Lin B, Ma M, Liang X, Li X, Lv W, *et al*: CircCD44 plays oncogenic roles in triple-negative breast cancer by modulating the miR-502-5p/KRAS and IGF2BP2/Myc axes. Mol Cancer 20: 138, 2021.
15. Li Z, Spoelstra NS, Sikora MJ, Sams SB, Elias A, Richer JK, Lee AV and Oesterreich S: Mutual exclusivity of ESR1 and TP53 mutations in endocrine resistant metastatic breast cancer. NPJ Breast Cancer 8: 62, 2022.
16. Lukianova N, Zadvornyi T, Kashuba E, Borikun T, Mushii O and Chekhun F: Expression of markers of bone tissue remodeling in breast cancer and prostate cancer cells in vitro. Exp Oncol 44: 39-46, 2022.
17. Yin Z, Wang W, Qu G, Wang L, Wang X and Pan Q: MiRNA-96-5p impacts the progression of breast cancer through targeting FOXO3. Thorac Cancer 11: 956-963, 2020.
18. Peng D, Fu M, Wang M, Wei Y and Wei X: Targeting TGF-β signal transduction for fibrosis and cancer therapy. Mol Cancer 21: 104, 2022.
19. Shi X, Yang J, Deng S, Xu H, Wu D, Zeng Q, Wang S, Hu T, Wu F and Zhou H: TGF-β signaling in the tumor metabolic microenvironment and targeted therapies. J Hematol Oncol 15: 135, 2022.
20. Richard V, Davey MG, Annuk H, Miller N and Kerin MJ: The double agents in liquid biopsy: Promoter and informant biomarkers of early metastases in breast cancer. Mol Cancer 21: 95, 2022.
21. San A, Palmieri D, Saxena A and Singh S: In silico study predicts a key role of RNA-binding domains 3 and 4 in nucleolin-miRNA interactions. Proteins 90: 1837-1850, 2022.
22. Sirkisoon SR, Wong GL, Aguayo NR, Doheny DL, Zhu D, Regua AT, Arrigo A, Manore SG, Wagner C, Thomas A, *et al*: Breast cancer extracellular vesicles-derived miR-1290 activates astrocytes in the brain metastatic microenvironment via the FOXA2→CNTF axis to promote progression of brain metastases. Cancer Lett 540: 215726, 2022.
23. Søiland H, Janssen EAM, Helland T, Eliassen FM, Hagland M, Nordgård O, Lunde S, Lende TH, Sagen JV, Tjensvoll K, *et al*: Liquid biopsies and patient-reported outcome measures for integrative monitoring of patients with early-stage breast cancer: A study protocol for the longitudinal observational prospective breast cancer biobanking (PBCB) study. BMJ OPen 12: e054404, 2022.
24. Storci G, De Carolis S, Papi A, Bacalini MG, Gensous N, Marasco E, Tesei A, Fabbri F, Arienti C, Zanoni M, *et al*: Genomic stability, anti-inflammatory phenotype and up-regulation of the RNAseH2 in cells from centenarians. Cell Death Differ 26: 1845-1858, 2019.
25. Kang, J. Li Y, Zou Y, Zhao Z, Jiao L and Zhang H: miR-96-5p induces orbital fibroblasts differentiation by targeting Smad7 and promotes the development of thyroid-associated ophthalmopathy. Evid Based Complement Alternat Med: Feb 27, 8550307, 2022.
26. Chao L, Hua-Yu Z, Wen-Dong B, Mei S, Bin X, Da-Hai H and Yi L: miR-96 promotes collagen deposition in keloids by targeting Smad7. Exp Ther Med 17: 773-781, 2019.
27. Shi Y, Zhao Y, Shao N, Ye R, Lin Y, Zhang N, Li W, Zhang Y and Wang S: Overexpression of microRNA-96-5p inhibits autophagy and apoptosis and enhances the proliferation, migration and invasiveness of human breast cancer cells. Oncol Lett 13: 4402-4412, 2017.
28. Uehiro N, Horii R, Iwase T, Tanabe M, Sakai T, Morizono H, Kimura K, Iijima K, Miyagi Y, Nishimura S, *et al*: Validation study of the UICC TNM classification of malignant tumors, seventh edition, in breast cancer. Breast Cancer 21: 748-753, 2014.
29. Livak KJ and Schmittgen TD: Analysis of relative gene expression data using real-time quantitative PCR and the 2(-Delta Delta C(T)) method. Methods 25: 402-408, 2001.
30. Farstad W: Ethics in animal breeding. Reprod Domest Anim 53 (Suppl 3): S4-S13, 2018.
31. Percie du Sert N, Hurst V, Ahluwalia A, Alam S, Avey MT, Baker M, Browne WJ, Clark A, Cuthill IC, Dirnagl U, *et al*: The ARRIVE guidelines 2.0: Updated guidelines for reporting animal research. PLoS Biol 18: e3000410, 2020.
32. Tan L, Mai D, Zhang B, Jiang X, Zhang J, Bai R, Ye Y, Li M, Pan L, Su J, *et al*: PIWI-interacting RNA-36712 restrains breast cancer progression and chemoresistance by interaction with SEPW1 pseudogene SEPW1P RNA. Mol Cancer 18: 9, 2019.
33. Tang H, Huang X, Wang J, Yang L, Kong Y, Gao G, Zhang L, Chen ZS and Xie X: circKIF4A acts as a prognostic factor and mediator to regulate the progression of triple-negative breast cancer. Mol Cancer 18: 23, 2019.
34. Barzaman K, Karami J, Zarei Z, Hosseinzadeh A, Kazemi MH, Moradi-Kalbolandi S, Safari E and Farahmand L: Breast cancer: Biology, biomarkers, and treatments. Int Immunopharmacol 84: 106535, 2020.
35. Bahreini F, Rayzan E and Rezaei N: microRNA-related single-nucleotide polymorphisms and breast cancer. J Cell Physiol 236: 1593-1605, 2021.
36. Wang Y and Li C: lncRNA GHET1 promotes the progression of Triple-Negative breast cancer via regulation of miR-377-3p/GRSF1 signaling axis. Comput Math Methods Med 2022: 8366569, 2022.
37. Weng YS, Tseng HY, Chen YA, Shen PC, Al Haq AT, Chen LM, Tung YC and Hsu HL: MCT-1/miR-34a/IL-6/IL-6R signaling axis promotes EMT progression, cancer stemness and M2 macrophage polarization in triple-negative breast cancer. Mol Cancer 18: 42, 2019.
38. Liu B, Zhang J and Yang D: miR-96-5p promotes the proliferation and migration of ovarian cancer cells by suppressing Caveolae1. J Ovarian Res 12: 57, 2019.
39. Zhou J, Sun X, Zhang X, Yang H, Jiang Z, Luo Q, Liu Y and Wang G: miR-107 is involved in the regulation of NEDD9-mediated invasion and metastasis in breast cancer. BMC Cancer 22: 533, 2022.
40. Zhou Y, Cai W and Lu H: Overexpression of microRNA-145 enhanced docetaxel sensitivity in breast cancer cells via inactivation of protein kinase B gamma-mediated phosphoinositide 3-kinase-protein kinase B pathway. Bioengineered 13: 11310-11320, 2022.
41. Yan W, Cao M, Ruan X, Jiang L, Lee S, Lemanek A, Ghassemian M, Pizzo DP, Wan Y, Qiao Y, *et al*: Cancer-cell-secreted miR-122 suppresses O-GlcNAcylation to promote skeletal muscle proteolysis. Nat Cell Biol 24: 793-804, 2022.
42. Yang R, Xing L, Zheng X, Sun Y, Wang X and Chen J: The circRNA circAGFG$_1$ acts as a sponge of miR-195-5p to promote triple-negative breast cancer progression through regulating CCNE1 expression. Mol Cancer 18: 4, 2019
43. Arase M, Horiguchi K, Ehata S, Morikawa M, Tsutsumi S, Aburatani H, Miyazono K and Koinuma D: Transforming growth factor-β-induced lncRNA-Smad7 inhibits apoptosis of mouse breast cancer JygMC(A) cells. Cancer Sci 105: 974-982, 2014.
44. Kong X, Yan K, Deng P, Fu H, Sun H, Huang W, Jiang S, Dai J, Zhang QC, Liu JG and Xi Q: LncRNA-Smad7 mediates cross-talk between Nodal/TGF-β and BMP signaling to regulate cell fate determination of pluripotent and multipotent cells. Nucleic Acids Res 50: 10526-10543, 2022.
45. Gao X, Cao Y, Yang W, Duan C, Aronson JF, Rastellini C, Chao C, Hellmich MR and Ko TC: BMP2 inhibits TGF-β-induced pancreatic stellate cell activation and extracellular matrix formation. Am J Physiol Gastrointest Liver Physiol 304: G804-G813, 2013.
46. Tang PC, Zhang YY, Li JS, Chan MK, Chen J, Tang Y, Zhou Y, Zhang D, Leung KT, To KF, *et al*: LncRNA-Dependent mechanisms of transforming growth Factor-β: From tissue fibrosis to cancer progression. Noncoding RNA 8: 36, 2022.
47. Luo L, Li N, Lv N and Huang D: SMAD7: A timer of tumor progression targeting TGF-β signaling. Tumour Biol 35: 8379-8385, 2014.
48. Zhong C, Xie Z, Shen J, Jia Y and Duan S: LINC00665: An emerging biomarker for cancer diagnostics and therapeutics. Cells 11: 1540, 2022.
49. Qin WY, Feng SC, Sun YQ and Jiang GQ: MiR-96-5p promotes breast cancer migration by activating MEK/ERK signaling. J Gene Med 22: e3188, 2020.
50. Luo X, Zhang D, Xie J, Su Q, He X, Bai R, Gao G and Pan W: MicroRNA-96 promotes schistosomiasis hepatic fibrosis in mice by suppressing smad7. Mol Ther Methods Clin Dev 11: 73-82, 2018.